Optimization of the Crest Factor for Complex-Valued Multisine Signals

Bence CSEPPENTO [1], Andras RETZLER [1,2,3], Zsolt KOLLAR [1]

[1] Dept. of Measurement and Information Systems, Budapest University of Technology and Economics, Műegyetem rkp. 3, H-1111, Budapest, Hungary
[2] Dept. of Mechanical Engineering and DMMS-M Core Lab, KU Leuven, Celestijnenlaan 300, B-3001, Heverlee, Belgium
[3] Flanders Make@KU Leuven, B-3001, Leuven, Belgium

cseppento@mit.bme.hu

Submitted March 16, 2023 / Accepted May 4, 2023 / Online first May 17, 2023

Abstract. *Multisine signals are commonly used in the measurement of dynamic systems and wireless channels. For optimal measurements with a high dynamic range, a low Crest Factor (CF) excitation signal is required. In this paper, a modified approach to optimize the crest factor for complex-valued multisine signals is presented. The approach uses a nonlinear optimization method where the real and imaginary parts can also be optimized for low CF. Furthermore, extensions of the real-valued multisine CF optimization methods are presented for complex-valued cases. The proposed methods are validated and compared using simulations. Based on the results it is shown that the novel approach can lead to more optimal signal design and lower CF compared to other techniques for complex-valued multisine signals.*

Keywords

Multisine, crest factor, PAPR, optimization, complex signal, channel estimation, OFDM

1. Introduction

The optimal design of test and measurement signals is a key factor for analyzing and identifying mechanical systems, biomedical systems, batteries, or for measuring wireless transmission channels. Identification of the plant model is the first step before a suitable control algorithm can be developed. In the case of wireless communication, the estimation of the radio channel is essential before a channel equalization method can be applied to reconstruct the transmitted data.

To identify the time-domain impulse response, and frequency-domain transfer function of a system under observation certain excitation signals have to be applied. Furthermore, the identification of nonlinearities present in the system might also be a preferable task. Restrictions in both time- and frequency-domain lead to constraints that are not straightforward to fulfill during the design process of the excitation signal.

An ideal Dirac impulse is not realizable in practical systems. Applying such an impulse-shaped function might also be destructive for the system under observation. Such excitation signals are commonly used in mechanical or acoustic systems using impact hammers [1]. Another commonly used excitation function in system identification is the Heaviside step function. It is also hard to approximate, and it might not be the best choice in the case of bandlimited systems. Depending on the limitation posed by the system on the input signal, other signals can also be applied: in case of binary input systems pseudorandom binary sequence [2] or in case of bandlimited systems, chirp [3] or multisine [4] signals can be used.

In this paper, we focus on multisine excitation signals as they have flat and well-localized spectra, and they are especially suitable for frequency domain identification purposes [5]. The generation and processing of such signals can be efficiently performed by applying Fast Fourier Transform (FFT) and Inverse FFT (IFFT).

Multisine test signals are used in various applications, such as testing of analog integrated circuits [6], electric drivetrains [7], impedance spectroscopy [8], [9], battery diagnosis [10], vibration analysis of bridges [11], or even wireless channel estimation [12], [13].

Multisine signals can be designed in a comfortable manner to measure the dedicated bandwidth of the system with constant amplitude spectra. As the time-domain signal is a sum of many sinusoids, it has a noise-like amplitude distribution. This phenomenon can be controlled by selecting the phase values of the components to minimize the amplitude fluctuation of the resultant signal.

Numerous techniques have been proposed for determining or optimizing the phase values of the frequency components to achieve a low amplitude fluctuation of the

DOI: 10.13164/re.2023.0264

time-domain signal, i.e. Crest Factor (CF). A closed-form expression for the phase values was introduced in [14], which results in moderate CF values. Various iterative time-frequency-domain swapping algorithms were proposed by [15–18]. An optimization technique, namely using the nonlinear Chebyshev approximation method, was given in [19]. An application of the Artificial Bee Colony (ABC) algorithm was presented by [20]. Recently, a nonlinear optimization method [4] was proposed, which can achieve the best performance among the compared methods. This method is based on the algorithm presented in [19] using an interior-point solver, then improves the result by utilizing a slack variable.

The relevance of examining complex-valued multisines is mainly applicable to Orthogonal Frequency Division Multiplexing (OFDM) signals used for wireless communication, for which a low CF of the real and imaginary parts and for the modulated signal is desired. In the past decades algorithms for CF reduction have been proposed [21], [22].

In this paper, we propose an optimization algorithm based on Guillaume's method [19], whose cost function is the weighted sum of the CF and the CF of the real and imaginary parts. Additionally, Yang's method [18] has been generalized for complex signals and can optionally be applied after each p-norm iteration of Guillaume's method. The algorithm has been tested with a number of weights in the cost function, and with or without using the swapping method. For the simulations, we have considered multisine signals with equi-flat spectra comprising moderate (31) and high (1000) number of tones.

The paper is organized as follows. In the next section, the multisine excitation signal is defined and the generation steps are described. Furthermore, the metrics to determine the amplitude fluctuations are given. Section 3 presents an overview of the most important CF minimization algorithms found in the literature. In Sec. 4, improved CF minimization algorithms for complex multisine signals are described. Section 5 presents the simulation results. A statistical comparison of the proposed methods with the other methods is shown in terms of the achievable CF. In the final section, the conclusions are drawn.

2. Multisine Signals

The time-domain samples – with normalized sampling time – of complex multisines are defined as

$$x[n] = \sum_{k=1}^{K} C_k \mathrm{e}^{\mathrm{j}2\pi f_k n} \tag{1}$$

without a DC component, represented by the term $k = 0$, where K is the number of complex-valued frequency components in the multisine signal. C_k and f_k are the complex amplitude and frequency of the k^{th} component. The complex amplitude C_k can be expressed as:

$$C_k = |C_k| \mathrm{e}^{\mathrm{j}\varphi_k} \tag{2}$$

where $|C_k|$ is the amplitude and $\varphi_k = \angle C_k$ is the phase of the k^{th} tone.

In order to generate periodic multisine signals with a period of N samples, the normalized frequencies should be chosen as $f_k = k/N$. This way the frequencies are spaced equidistantly. Furthermore, this choice of frequencies enables the synthesis and analysis of multisine signals efficiently with low computational complexity using the IFFT and FFT algorithms, respectively.

Complex-valued multisine signals are typically applied in wireless communication systems where the transmission is done in the passband and the radio channel is measured at a certain transmission frequency with limited bandwidth. After the D/A conversion an analog low-pass filter is needed to remove the high-frequency components inherently added by the conversion. Then an In-phase and Quadrature-phase (IQ) modulator is used to modulate the signal. The block diagram of a measurement setup using complex-valued multisine signal is shown in Fig. 1. In the case of the complex-valued multisine signals, the real and imaginary parts are created and filtered separately before modulating it with a sine and a cosine version of the carrier wave (f_c). After modulation, the two paths are added, and a High Power Amplifier (HPA) is applied to amplify the signal in the passband before transmitting it using an antenna over the radio channel.

A real-valued multisine signal is a special case of (1) when the following holds:

$$C_k = C_{N-k}^{*} \tag{3}$$

where C^* denotes the complex conjugate of C. The resulting real-valued multisine signal may be expressed as

$$x[n] = \sum_{k=1}^{K} A_k \cos(2\pi f_k n + \varphi_k) \tag{4}$$

where K is the number of frequencies, $A_k = 2|C_k|$, f_k and φ_k are the amplitude, frequency and initial phase of the k^{th} frequency. Note that in the case of a real-valued multisine signal of K tones, there are $2K$ non-zero components in the spectrum, due to the complex conjugate symmetry given by (3).

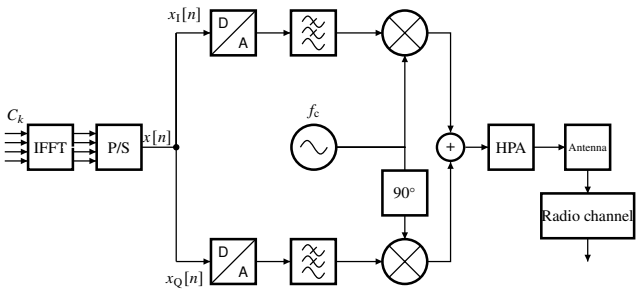

Fig. 1. Measurement setup of a radio channel using complex-valued multisine signal applying an IQ modulator.

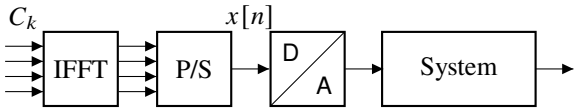

Fig. 2. Measurement setup of a system using a real-valued multisine signal.

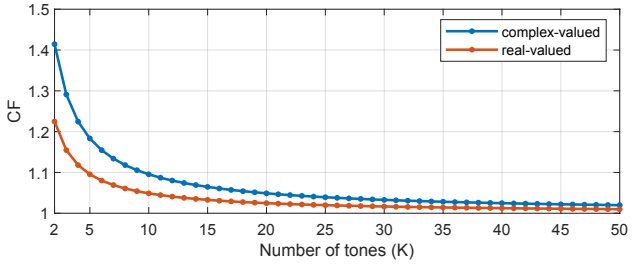

Fig. 3. Theoretical lower limit of the crest factor for real- and complex-valued multisine signals.

Real-valued multisine signals are used in a wider area such as mechanical, electrical, chemical or biomedical systems where the excitation signal is applied in the baseband. After generating the signal in the frequency domain, the time-domain data is acquired using the IFFT algorithm. Then a Parallel-to-Series converter (P/S) feeds the data to a Digital-to-Analog (D/A) converter to acquire a time-domain signal for the excitation of the investigated system as shown in Fig. 2.

The Crest Factor (CF) of a signal is defined as the ratio of the maximum value and the Root Mean Square (RMS) of the signal:

$$\mathrm{CF(x)} = \frac{\max\left(|x|\right)}{\mathrm{RMS}(x)} = \frac{\max\left(|x[n]|\right)}{\sqrt{\frac{1}{N}\sum\limits_{n=1}^{N}|x[n]|^2}}. \tag{5}$$

In terms of complex-valued signals, such as modulated radio transmission signals, the notion of Peak-to-Average Power Ratio (PAPR) is often used:

$$\mathrm{PAPR} = 20\log_{10}(\mathrm{CF}). \tag{6}$$

Note that in (1) there is no DC component present, as the DC component would only manifest as an additional term in the peak value and the square of the RMS, increasing the CF and the PAPR of the signal.

In the past decades, a number of approaches have been presented in order to minimize the crest factor, most of them dealing with the real-valued case [4, 15–19] – which is also relevant in the case of complex multisine signals as the I and Q channels are handled by separate D/A converters and mixers.

Besides generalizing an algorithm for complex-valued multisines, Friese [17] also dealt with the lower and upper bounds of the CF that can be achieved. It stands to reason that in case of a flat spectrum, i.e. the amplitude of each tone in the frequency-domain is equal, the CF is at most $\sqrt{K}$ as the RMS of the signal is $\sqrt{K}$, while the peak value is K in the worst case, if all tones are in phase.

Through calculations, [17] also defines a theoretical lower bound in the case of complex multisine signals containing more than one tone:

$$\mathrm{CF} \geq \sqrt{\frac{K+2}{K}} = \sqrt{1+\frac{2}{K}}. \tag{7}$$

For a large number of tones the boundary converges to 1, implicating that because for a smaller number of tones the number of variables is lower, the CF can not be decreased as much. This theoretical limit holds for any multisine signal; as a real-valued multisine is a special case, the formula also defines a lower limit as $\sqrt{1+\frac{1}{K}}$, however, the restriction defined in (3) is not taken into consideration. In the sequel, we are dealing exclusively with flat spectra, which is also not considered in [17]. Hence, it is a fair assumption that the theoretical lower limit will not be reached in either case. The limits for both real and complex cases are illustrated in Fig. 3.

A fast and simple approach for generating multisine signals with low CF is to run Monte-Carlo simulations with a set of randomly chosen phases and from the various realizations, the record with the lowest CF is selected for the measurement. In the case of $K = N$ tones, the worst-case value of the CF = N can be reached if all phases are identical, this way a time domain impulse is generated. Thus, for a large number of tones finding a set of phases that result in low CF might be computationally exhaustive. In the next section, various methods are presented which can efficiently reduce the CF/PAPR of multisine signals with a set of initial phases.

3. CF and PAPR Reduction Methods

3.1 Direct Calculation Methods

A closed-form formula – in case of flat spectra – for the phase values has been presented by Schroeder [14]:

$$\varphi_k = \pi\frac{(k-1)^2}{K}. \tag{8}$$

The main advantage of this method is that the phase values are calculated directly. Although the attainable crest factor reduction is only moderate compared to other iterative algorithms, it may also provide the initialization for other optimization techniques.

Other direct methods are also present in literature, such as the Newman multitone [23] for which the phases are given by the same formula as (8), but a lower crest factor is achieved by applying a non-flat amplitude spectrum. Furthermore, the application of Shapiro-Rudin phases [24] can result in a crest factor always lower than 2, but usually slightly higher than what is achievable using Newman phases. The phase values are defined as a binary sequence of the values 1 and −1, but the method has limitations when applying it to multisine signals with a large number of components.

3.2 Time-Frequency-Domain Swapping Methods

The processing steps of a heuristic method using iterative time-frequency-domain swapping are described in Algorithm 1.

Algorithm 1. Time-frequency-domain swapping algorithm

$i = 0$
while $\mathrm{CF}(x) > \mathrm{CF}_{\mathrm{target}}$ && $i \leq i_{\max}$ **do**
  $x'[n] = \mathrm{amplitude\_manip}(x[n])$
  $C'_k = \mathrm{FFT}(x'[n])$
  $C_k^i = \left|C_k^0\right| \mathrm{e}^{\mathrm{j}\angle C'_k}$
  $x[n] = \mathrm{IFFT}\left(C_k^i\right)$
  $i = i + 1$
end while
Require: $x[n], C_k^0, \mathrm{CF}_{\mathrm{target}}, i_{\max}$
return $x[n]$

First, initial values C_k^0 for the complex amplitude values of the multisine tones are selected. The IFFT is applied to form the time domain samples $x[n]$. Then, an iterative process starts, and this loop is repeated until the maximum number of iterations $i_{\max}$ are reached or the desired CF limit $\mathrm{CF}_{\mathrm{target}}$ is achieved. In each iteration, a new signal $x'[n]$ with manipulated time domain samples is formed. The FFT is used to calculate the modified complex amplitude values C'_k. The phase values of this signal are kept and the amplitude values are restored to the original values. Finally, using the new complex amplitude values C_k^i, a new time-domain signal is generated using the IFFT.

In general, the problem with such algorithms is that their convergence is hard to prove and the required number of iterations is hard to determine. In the following part, the various amplitude manipulation functions found in the literature are discussed briefly.

Following the observation that the signals with binary values have minimal CF, van den Bos [15] described a method to obtain better CF than the previously used Schroeder's method. The sign function is proposed as a time domain manipulation function, i.e.:

$$x'[n] = \mathrm{sign}(x[n]). \tag{9}$$

As a result, the signal $x'[n]$ will have only the amplitude values of -1 or 1. An additional stop criterion is proposed to the algorithm: if the phases do not change from one iteration to the next, the iterative process should stop.

Another amplitude manipulation method was proposed by van der Ouderaa [16]. In his algorithm, the time-domain signal is limited to a constant value of

$$A_{\mathrm{L}} = a_{\mathrm{L}} \cdot \max(|x[n]|) \tag{10}$$

with $a < 1$. The resulting amplitude manipulation function can be expressed as

$$x'[n] = \begin{cases} x[n], & \text{if } |x[n]| \leq A_{\mathrm{L}} \\ A_{\mathrm{L}}, & \text{if } |x[n]| > A_{\mathrm{L}} \end{cases}. \tag{11}$$

Based on experimental validation the optimal value for a_{L} lies between 0.75 and 0.95. Smaller values of a_{L} may cause divergence of the algorithm, while higher values of a_{L} lead to undesirably slow convergence.

Yang [18] proposed further improvement to the previous method by iteratively changing the value of a in (10) over the number of iterations. The best results have been found with a limit changing in a logarithmic manner as

$$a_{\mathrm{L}}(i) = \frac{\log_{10}(i + b_1)}{\log_{10}(b_2)} \tag{12}$$

where i is the iteration number, b_1 and b_2 are constants dependent on the desired CF.

3.3 Optimization Methods

The general aim of optimization is to find a set of phases minimizing (5) systematically instead of the heuristic methods described by Algorithm 1.

Local minimum search algorithms solve an optimization problem using a gradient-based method, for which a differentiable cost function is required. The state-of-the-art method for crest factor minimization is that of Guillaume et al. [19]. As the Chebyshev-norm (ℓ_∞-norm) is a non-differentiable function, the presented method approximates the peak value by an ℓ_p-norm. In the case of flat spectra, the ℓ_2-norm is constant, hence minimizing the peak value minimizes the CF as well. The method iteratively solves the optimization problem of minimizing the ℓ_p-norm, increasing the value of p, which is chosen as powers of 2, after each solve. The main advantage of the method is the improved reduction of the CF compared to time-frequency swapping algorithms; the disadvantage is that as in the case of any gradient-based method, it is not guaranteed that the global minimum is found. The algorithm presented in [4] enhanced Guillaume's method by subsequently solving another optimization problem, where the elements of a slack variable vector are minimized, while the absolute value of the time-domain samples of the signal are required to be less than the slack variable via an inequality constraint.

Global minimum search is possible using e.g. genetic, Particle Swarm Optimization (PSO) or Artificial Bee Colony (ABC) algorithms. An example of the latter was presented by Janeiro et al. in [20]. In the ABC algorithm, a number of candidate solutions are present, which are perturbed (i.e. the sets of initial phases are modified), then evaluated to determine whether the change resulted in a reduction of CF. At certain intervals, candidate solutions that were not improved are abandoned to be replaced by the currently best candidate (to improve chances of finding a local minimum by perturbing that candidate more times in an iteration) and new random candidates (to improve the chances of initialization close to another local minimum). A disadvantage of these global methods is the memory requirement, computational load and slow convergence in case of a large number of harmonics.

4. Proposed Methods for CF Optimization of Complex-Valued Multisines

In order to minimize the crest factor of complex-valued multisines, in addition to giving a theoretical lower bound, Friese [17] also developed a generalized time-frequency-domain swapping method overcoming the lack of definition of relations for complex numbers by defining a complex error signal to be subtracted from the signal in each iteration. To reduce the PAPR of OFDM signals, notable contributions were developed by Armstrong [22], whose method includes clipping the absolute value of the complex time-domain values, then applying time-dependent frequency-domain filtering to keep the transmitted data on a symbol-by-symbol basis; as well as by Tellado and Cioffi [21], who developed an optimization algorithm for determining a time-domain vector to be added to the signal in order to reduce PAPR, and also optimizing some carriers that are not transmitting data.

We suggest modifications to time-frequency-domain swapping algorithms and Guillaume's method for complex-valued multisines which optimize CF using all tones, i.e. in terms of OFDM signals we ignore data and rather acquire relative phase shifts between the tones in order to reduce PAPR.

A heuristic and simple approach is to clip the absolute value of the complex values in the time-domain while keeping the phase. As a result, the clipping algorithms presented in (11) have to be modified to keep the phases for complex signals as:

$$x'_{\mathrm{c}}[n] = \begin{cases} x[n], & \text{if } |x[n]| \leq A_{\mathrm{L}} \\ A_{\mathrm{L}} \mathrm{e}^{\mathrm{j}\angle x[n]}, & \text{if } |x[n]| > A_{\mathrm{L}} \end{cases}. \tag{13}$$

In wireless applications using complex multisine signals for measurement, the real and imaginary parts of the complex baseband signal are handled separately as shown in Fig. 1. As a result, it is worthwhile to minimize the crest factors of the I and Q components ($x_{\mathrm{I}}[n] = \Re\{x[n]\}$ and $x_{\mathrm{Q}}[n] = \Im\{x[n]\}$) and not only reduce the PAPR of the resultant complex signal after modulation.

During the investigations, two versions of Yang's method are used. In the first case, the swapping algorithm is applied to the absolute value of the complex time domain signal. In the second case, the method is applied to the real and imaginary parts, separately.

In the case of optimization methods, as an extension of Guillame's method, the cost function can be altered in order to minimize both the CFs of the channels and the overall PAPR at the same time. Modifying Guillaume's method, the proposed problem to be solved in an iterative manner can be given as

$$\underset{\varphi}{\text{minimize}} \sum_{n=0}^{N-1} \left(w_{\mathrm{I}} \left|\left|x_{\mathrm{I}}[n]\right|\right|_p + w_{\mathrm{Q}} \left\|x_{\mathrm{Q}}[n]\right\|_p + w \left|\left|x[n]\right|\right|_p \right) \tag{14}$$

where $||\cdot||_p$ denotes the p-norm. The method is versatile, as the weights (w_{I}, w_{Q}, w) can be tuned, and after each solution, minimization may be assisted by using a time-frequency-domain swapping algorithm as well. Guillaume's method is considered a special case, where $w_{\mathrm{I}} = w_{\mathrm{Q}} = 0$.

The main differences in comparison with the algorithm presented for real-valued multisines in [4] are the following:

- After iteratively solving (with increasing p) (14) for real signals, the algorithm of [4] consisted of solving another optimization problem which reduced time-domain fluctuations by using a slack variable – this is omitted.
- Instead, there is an option to use a time-frequency-domain swapping algorithm after each solution of the optimization problem. For this purpose, Yang's algorithm is used.

5. Simulations

5.1 Proposed Algorithm

Both time-frequency-domain swapping and Guillaume's method are implemented for MATLAB in the Fdident toolbox [5], while the best performing swapping algorithm is that of Yang's using logarithmically changing clipping thresholds [18]. For flat spectra containing 31 and 100 harmonics, crest factors as low as 1.3750 and 1.3997 have been reported. The two methods may be combined such that after each iteration of the optimization problem, Yang's algorithm is executed, and the resulting signal is used before the next iteration with the increased p value. Another improvement of Guillaume's algorithm was proposed by Retzler et al. [4] by reformulating the optimization problem in MATLAB using CasADi [25] and such that instead of optimizing the phases, each tone is expressed as a sum of a cosine and sine signal, removing some of the nonlinearity of the cost function; then a second optimization problem is solved, attempting to lower the peak value via a slack variable. This algorithm decreased the CF of 31 and 100 tones to 1.3513 and 1.3512, respectively. To date, this method manages to outperform previous algorithms at the cost of increased computation time, except for the computation time of the ABC algorithm, which is the higher.

The proposed optimization algorithm for complex multisine signals (14) has been implemented in CasADi [25] using the open-source Ipopt solver [26]. It has been tested using a varied set of weights and three different versions with regards to combination with a swapping algorithm. The three investigated versions are the following:

- Version A: no swapping method is incorporated,
- Version B: Yang's algorithm is used after each solution of (14) with the modification shown in (13),
- Version C: after each solution of (14), Yang's algorithm is executed on both $x_{\mathrm{I}}[n]$ and $x_{\mathrm{Q}}[n]$, then $x'[n] = x'_{\mathrm{I}}[n] + \mathrm{j}x'_{\mathrm{Q}}[n]$ is constructed.

The set of used weights is shown in Tab. 1. The reason for this is to demonstrate how the algorithm behaves when either the overall CF or the CF of the I-Q channels is not taken into account, or either is over-weighted in the objective function.

5.2 Comparison of Results

In order to gauge the performance of the proposed versions and study the effect of the choice of weights, Monte Carlo simulations of 1024 test cases initialized with randomly generated φ_k values (using the same sets of values for each scenario) have been run on flat spectra containing 15, 31, and 100 equi-distant components. In all cases, to ensure proper oversampling so that the results are not distorted, the number of samples was $N = 4096$, while p was increased from 4 to 128. The simulations were run on a virtual machine of 16 CPU cores (for parallelization of the test cases) and 64GB of RAM. The bottleneck of the algorithms is the memory requirement, as for multitone signals of 1000 carriers approximately 2.5GB of RAM is required in the case of the proposed optimization method.

The results for a multisine with 31 tones are presented in Tab. 2. Three scenarios have been highlighted in bold: Guillaume's algorithm generalized for complex signals, Guillaume's algorithm enforced by a swapping method between iterations and a case when CF_I and CF_Q are over-weighted. Based on the presented table, a number of conclusions can be inferred. Firstly, the results do not vary depending on which version of Yang's method is used (version B or C), as attempting to minimize the CF inherently causes a decrease in CF_I and CF_Q as well. The cases with $\begin{bmatrix} w_I & w_Q & w \end{bmatrix} = \begin{bmatrix} 1 & 1 & 0 \end{bmatrix}$ produce the highest CFs, as the real and imaginary parts are optimized separately and no attention is given to overall CF in the objective function. Secondly, if an application requires low CF_I and CF_Q, it can be achieved by weighting these in the objective function of the optimization at the cost of an increase in overall CF. The difference between the versions and weight sets is marginal, but note that the best result occurred in the case of version B, $\begin{bmatrix} w_I & w_Q & w \end{bmatrix} = \begin{bmatrix} 10 & 10 & 1 \end{bmatrix}$. Version A, $\begin{bmatrix} w_I & w_Q & w \end{bmatrix} = \begin{bmatrix} 0 & 0 & 1 \end{bmatrix}$ is also highlighted as this case corresponds to Guillaume's method.

w_I	w_Q	w
1	1	1
1	1	0
0	0	1
10	10	1
1	1	10

Tab. 1. List of weight combinations used in (14).

Version	w_I; w_Q; w	Mean CF_I	Mean CF_Q	Mean CF	Avg. time [s]
A	1; 1; 1	1.5810	1.5798	1.1655	39.7
A	1; 1; 0	1.5634	1.5617	1.2727	36.1
A	**0; 0; 1**	**1.6098**	**1.6096**	**1.1442**	**33.2**
A	10; 10; 1	1.5672	1.5665	1.2438	35.5
A	1; 1; 10	1.6052	1.6038	1.1483	36.6
B	1; 1; 1	1.5796	1.5787	1.1646	43.7
B	1; 1; 0	1.5611	1.5593	1.2704	42.5
B	**0; 0; 1**	**1.6077**	**1.6075**	**1.1426**	**39.0**
B	**10; 10; 1**	**1.5619**	**1.5607**	**1.2387**	**42.5**
B	1; 1; 10	1.6001	1.6004	1.1451	43.1
C	1; 1; 1	1.5807	1.5797	1.1658	37.7
C	1; 1; 0	1.5640	1.5613	1.2723	37.0
C	0; 0; 1	1.6118	1.6128	1.1461	34.1
C	10; 10; 1	1.5664	1.5660	1.2417	36.4
C	1; 1; 10	1.6022	1.6024	1.1465	37.0

Tab. 2. Mean CF values, and average computation time for 31 tones in each version with each set of weights.

A comparison of Yang's algorithm, defined by Algorithm 1 and (13), Guillaume's method, Guillaume's method combined with Yang's method, and a weighted optimization is shown in Fig. 4. The boxplots represent the statistics of the 1024 test cases of the Monte Carlo simulation: the horizontal bounds of the boxes represent the 25th and 75th percentiles: the red line in each box represents the median, the whiskers represent the interval in which results are not considered outliers, while the red crosses are the outliers.

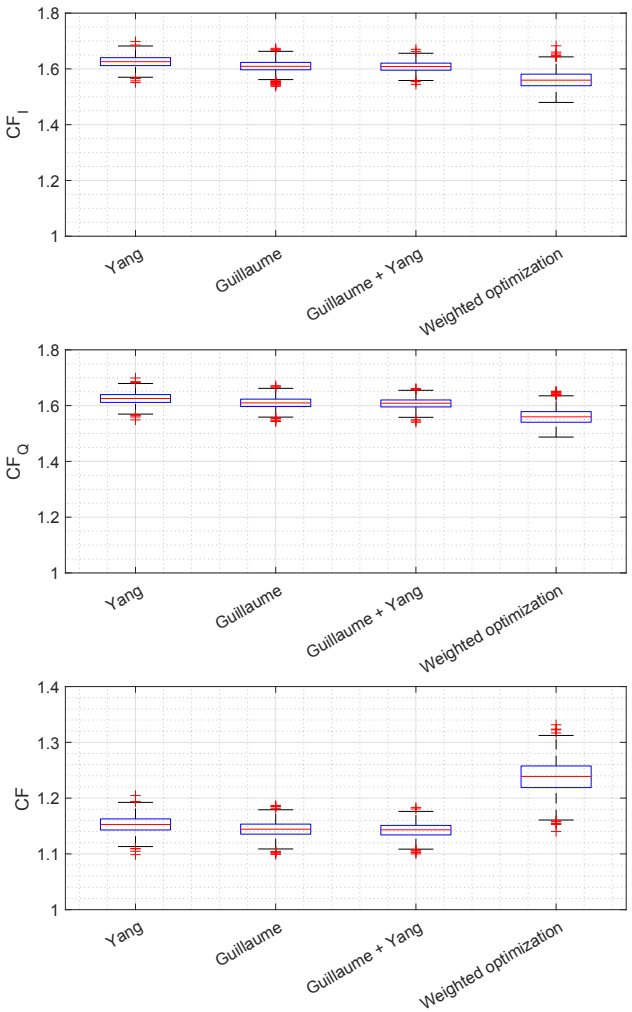

Fig. 4. Comparison of CF_I, CF_Q and CF in the case of 31 tones for different algorithms.

In Fig. 4, comparing Guillaume's method combined with Yang's and the weighted optimization illustrates the trade-off introduced by the weights between CF and CF_I and CF_Q. The boxplots illustrate the conclusions drawn from Tab. 2:

- a significant reduction of CF is achieved by Guillaume's method,
- the incorporation of Yang's method gives a slight advantage,
- overweighting CF_I and CF_Q results in lower CF of the real and imaginary parts at the cost of increasing the overall CF.

A comparison between existing methods is made difficult as in terms of complex signals, previous literature [17, 21, 22] did not impose a constraint on the shape of the amplitude spectrum, while we deal with signals with flat spectra. However, CF_I and CF_Q may be compared to CFs acquired for real-valued multisines. For the same configuration [4] achieved an average CF of 1.4041, while our result is in the range between 1.561 and 1.562 if the CFs of the I- and Q-components are given a higher weight. The difference is present in a smaller part because of our oversampling ($N = 4096$ as opposed to $N = 2048$), and in a larger part due to the fact that we also optimize for overall CF which is not present in the real-valued case.

To verify the relevance of the method for signals with a larger number of tones, test cases with 1000 components were also examined. For these signals, $N = 2048$ was used. The comparison for 1000 tones is shown in Tab. 3 for a smaller assortment of versions and weights chosen based on the results of the 31-tone case. Once again, the lowest CF is achieved by using Guillaume's algorithm, however, combining it with Yang's method decreases computation time by about 10%, as the swapping method jump-starts each iteration. As expected based on the results for 31 tones, adding increasing weights to CF_I and CF_Q can decrease the CF of the real and imaginary parts at the cost of overall CF.

Figure 5 shows a comparison between Yang's algorithm, Guillaume's algorithm by itself or combined with Yang's algorithm, and a weighted optimization combined with Yang's algorithm. The graphs show that for a large number of tones, the advantage of optimization over the swapping algorithm is more pronounced due to the increased number of optimization variables: the CF reduction of the gradient-based methods is larger, and the variance is smaller than in the case of only using Yang's method. The small variance implies that obtaining an acceptable result does not depend on the random initialization of phases, hence the time-consuming algorithm needs to run only once with arbitrary initialization to provide a desirable result.

One method of demonstrating the scalability of the algorithm is analyzing the computation time. The average computation times for the proposed combined algorithm for different numbers of tones are shown in Tab. 4. The data show that in the case of the time-frequency-domain swapping method (Yang's algorithm) computation time increases linearly with the increase of K, while for any optimization method (either Guillaume's, or Guillaume's combined with Yang's algorithm), the increase in time is quadratic. As a consequence, the computation time of swapping methods scale better with the increase of tones, however, swapping methods provide a smaller reduction of the CF.

Version	w_I; w_Q; w	Mean CF_I	Mean CF_Q	Mean CF	Avg. time [min]
A	0; 0; 1	1.5316	1.5326	1.0860	625
B	1; 1; 1	1.3657	1.3679	1.2035	560
B	0; 0; 1	1.5314	1.5316	1.0860	550
B	10; 10; 1	1.3182	1.3197	1.3123	555

Tab. 3. Mean CF values for 1000 tones in selected versions.

Method \ Tones	15	31	100	1000
Yang abs	0.36 s	0.48 s	1.59 s	13.31 s
Guillaume	10.84 s	33.23 s	386 s	37600 s
Weighted optimization with swapping	20.21 s	42.52 s	400 s	33800 s

Tab. 4. Average computation time of the investigated algorithms for different numbers of complex multisine tones.

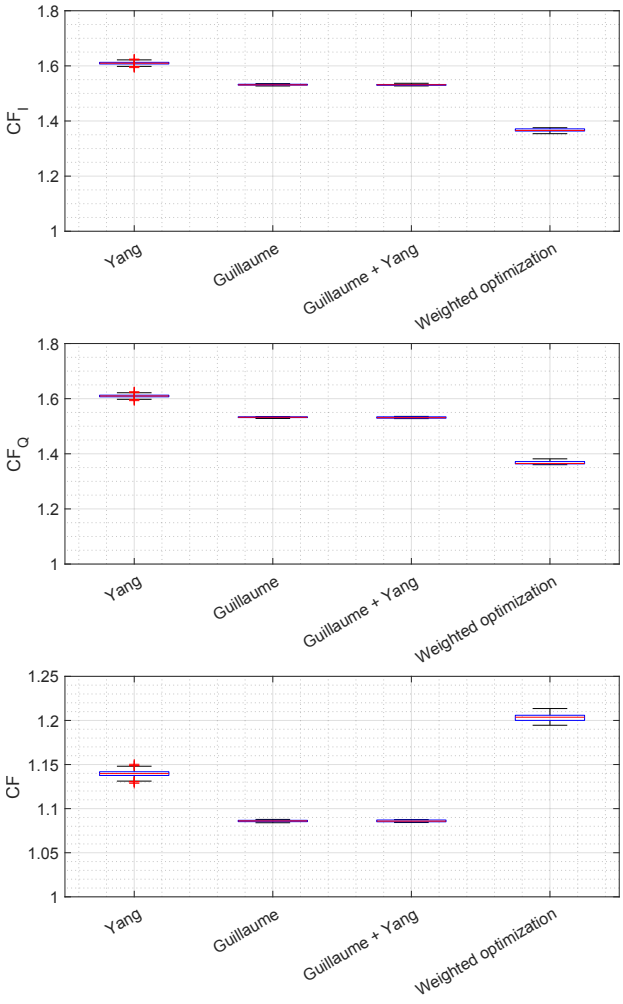

Fig. 5. Comparison of CF_I, CF_Q and CF in the case of 1000 tones for different algorithms.

6. Conclusion

In this paper, we have suggested methods for extending existing crest factor minimization methods for complex-valued multisine signals having equi-flat amplitude spectra. In the case of time-frequency domain swapping algorithms, two modifications are introduced: clipping the absolute value of samples in the time-domain while keeping the phase information, or executing the algorithm separately on the real and imaginary parts of the complex signal. The state–of–the–art method, Guillaume's algorithm, was extended for complex signals by including the options of not only optimizing for overall CF but for the CF of the real and imaginary parts as well, which can be advantageous in certain applications. Furthermore, we combined the optimization with a swapping algorithm.

The results show that the combination of Guillaume's optimization for p-norms and Yang's swapping algorithm for complex signals has the best results in terms of PAPR. It was also shown, that if minimizing the CF of the real and imaginary parts is crucial, the proposed objective function outperforms all other algorithms in this regard at the cost of an increase in overall CF or PAPR. Finally, it was shown that the proposed methods are also applicable to multisine signals of a large number of tones while maintaining a small variance with regard to the initialization of the phases.

The invariance regarding initialization is important, because as a consequence the optimization of CF needs to be run only once for a certain tone number and amplitude spectra, and the resulting signal may be reused for multiple applications, which is an advantage, as the computation time of the algorithm is rather high. In the future, it would be worthwhile to study CF_I, CF_Q, and PAPR if certain subcarriers in the OFDM signal are modulated with data. Furthermore, the possibility of real-time minimization is also an open issue, as the current solution is computationally complex, and computation time increases quadratically with respect to the number of tones.

Acknowledgments

The research reported in this paper was partially carried out at the Budapest University of Technology and Economics has been partially supported by the National Research, Development, and Innovation Fund of Hungary under Grant TKP2021-EGA-02 and by the National Research Development and Innovation Office (NKFIH) through the OTKA Grant K 142845.

This research was partially supported by Flanders Make: SBO project ROCSIS: Robust and Optimal Control of Systems of Interacting Subsystems, and ICON project ID2CON: Integrated IDentification for CONtrol. This work also benefits KU Leuven Center-of-Excellence Optimization in Engineering (OPTEC).

The research reported in this paper was partially carried out in the framework of the Gedeon Richter PhD scholarship of excellence by Gedeon Richter Talentum Foundation.

References

[1] BEREZVAI, S., KOSSA, A., BACHRATHY, D., et al. Numerical and experimental investigation of the applicability of pellet impacts for impulse excitation. *International Journal of Impact Engineering*, 2018, vol. 115, p. 19–31. DOI: 10.1016/j.ijimpeng.2018.01.006

[2] YADAV, E. S., INDIRAN, T. PRBS based identification and conditional control for an optimal operation of a pilot plant binary distillation column. In *8th International Conference on Modeling Simulation and Applied Optimization (ICMSAO)*. Manama (Bahrain), 2019, p. 1–5. DOI: 10.1109/ICMSAO.2019.8880422

[3] XIA, X. System identification using chirp signals and time-variant filters in the joint time-frequency domain. *IEEE Transactions on Signal Processing*, 1997, vol. 45, no. 8, p. 2072–2084. DOI: 10.1109/78.611210

[4] RETZLER, A., CSEPPENTŐ, B., SWEVERS, J. et al. Improved crest factor minimization of multisine excitation signals using nonlinear optimization. *Automatica*, 2022, vol. 146, p. 1–6. DOI: 10.1016/j.automatica.2022.110654

[5] KOLLÁR, I. *Frequency Domain System Identificaton Toolbox for MATLAB*. Budapest, 2004–2020. [Online]. Available at: http://home.mit.bme.hu/~kollar/fdident/

[6] SHIBASAKI, Y., ASAMI, K., KUWANA, A., et al. Crest factor controlled multi-tone signals for analog/mixed-signal IC testing. In *IEEE International Test Conference in Asia (ITC-Asia)*. Tokyo (Japan), 2019, p. 7–12. DOI: 10.1109/ITC-Asia.2019.00015

[7] TANTAU, M., PETERSEN, T., WIELITZKA, M., et al. Constrained design of multisine signals for frequency-domain identification of electric drive trains. *IFAC-PapersOnLine*, 2020, vol. 3, no. 2, p. 8750–8756. DOI: 10.1016/j.ifacol.2020.12.1369

[8] YE, X., JIANG, T., MA, Y., et al. A portable, low-cost and high-throughput electrochemical impedance spectroscopy device for point-of-care biomarker detection. *Biosensors and Bioelectronics: X*, 2023, vol. 13, p. 1–8. DOI: 10.1016/j.biosx.2022.100301

[9] ALTHOFF, H., EBERHARDT, M., GEINITZ, et al. Advances in crest factor minimization for wide-bandwidth multi-sine signals with non-flat amplitude spectra. *Computer Sciences & Mathematics Forum*, 2022, vol. 2, no. 1, p. 1–10. DOI: 10.3390/IOCA2021-10908

[10] DU, X., MENG, J., PENG, J., et al. A two-stage optimization framework for fast lithium-ion battery impedance measurement. *IEEE Transactions on Power Electronics*, 2023, vol. 38, no. 5, p. 5659–5664. DOI: 10.1109/TPEL.2023.3241072

[11] BOROŃ, P., DULIŃSKA, J. M., JASIŃKA, D. Advanced model of spatiotemporal mining-induced kinematic excitation for multiple-support bridges based on the regional seismicity characteristics. *Applied Sciences*, 2022, vol. 12, no. 14, p. 1–26. DOI: 10.3390/app12147036

[12] EISENBEIS, J., TINGULSTAD, M., KERN, N., et al. MIMO communication measurements in small cell scenarios at 28 GHz. *IEEE Transactions on Antennas and Propagation*, 2021, vol. 69, no. 7, p. 4070–4082. DOI: 10.1109/TApp.2020.3044394

[13] CSUKA, B., KOLLÁR, Z. Software and hardware solutions for channel estimation based on cyclic golay sequences. *Radioengineering*, 2016, vol. 25, no. 4, p. 801–807. DOI: 10.13164/re.2016.0801

[14] SCHRÖDER, M. Synthesis of low-peak-factor signals and binary sequences with low autocorrelation. *IEEE Transactions on Information Theory*, 1970, vol. 16, no. 1, p. 85–89. DOI: 10.1109/TIT.1970.1054411

[15] VAN DEN BOS, A. A new method for synthesis of low-peak-factor signals. *IEEE Transactions on Acoustics, Speech, and Signal Processing*, 1987, vol. 35, no. 1, p. 120–122. DOI: 10.1109/TASSP.1987.1165028

[16] VAN DER OUDERAA, E., SCHOUKENS, J., RENNEBOOG, J. Peak factor minimization using a time-frequency domain swapping algorithm. *IEEE Transactions on Instrumentation and Measurement*, 1988, vol. 37, no. 1, p. 145–147. DOI: 10.1109/19.2684

[17] FRIESE, M. Multitione signals with low crest factor. *IEEE Transactions on Communications*, 1997, vol. 45, no. 10, p. 1338–1344. DOI: 10.1109/26.634697

[18] YANG, Y., ZHANG, F., TAO, K., et al. An improved crest factor minimization algorithm to synthesize multisines with arbitrary spectrum. *Physiological Measurement*, 2015, vol. 36, no. 5, p. 895–910. DOI: 10.1088/0967-3334/36/5/895

[19] GUILLAUME, P., SCHOUKENS, J., PINTELON, R., et al. Crest-factor minimization using nonlinear Chebyshev approximation methods. *IEEE Transactions on Instrumentation and Measurement*, 1991, vol. 40, no. 6, p. 982–989. DOI: 10.1109/19.119778

[20] JANEIRO, F. M., HU, Y., RAMOS, P. M. Peak factor optimization of multiharmonic signals using artificial bee colony algorithm. *Measurement*, 2020, vol. 150, p. 1–8. DOI: 10.1016/j.measurement.2019.107040

[21] TELLADO, J., CIOFFI, J. M. Peak power reduction for multicarrier transmission. In *Global Telecommunications Conference*. Rio de Janeiro (Brazil), 1998, p. 951–955. DOI: 10.1109/GLOCOM.1999.829941

[22] ARMSTRONG, J. Peak-to-average reduction for OFDM by repeated clipping and frequency domain filtering. *IET Electronics Letters*, 2002, vol. 38, no. 5, p. 246–247. DOI: 10.1049/el:20020175

[23] BOYD, S. Multitone signals with low crest factor. *IEEE Transactions on Circuits and Systems*, 1986, vol. 33, no. 10, p. 1018–1022. DOI: 10.1109/TCS.1986.1085837

[24] POPOVIC, M. Synthesis of power efficient multitone signals with flat amplitude spectrum. *IEEE Transactions on Communications*, 1991, vol. 39, no. 7, p. 1031–1033. DOI: 10.1109/26.87205

[25] ANDERSSON, J. A. E., GILLIS, J., HORN, G., et al. CasADi: A software framework for nonlinear optimization and optimal control. *Mathematical Programming Computation*, 2019, vol. 11, no. 1, p. 1–36. DOI: 10.1007/s12532-018-0139-4

[26] WÄCHTER, A., BIEGLER, L. On the implementation of an interior-filter line-search algorithm for large-scale nonlinear programming. *Mathematical Programming*, 2006, vol. 106, no. 1, p. 25–57. DOI: 10.1007/s10107-004-0559-y

About the Authors ...

Bence CSEPPENTŐ obtained his M.Sc. degree in Electrical Engineering from the Budapest University of Technology and Economics (BME) in Hungary in 2019. He is currently pursuing a Ph.D. degree at BME, Hungary, under the supervision of Zsolt Kollár. His research topic focuses on model predictive control of nonlinear systems and optimization, while harboring an interest in digital signal processing, telecommunications, and microwave engineering.

András RETZLER obtained his B.Sc. and M.Sc. degrees in Electrical Engineering from Budapest University of Technology and Economics (BME), Hungary in 2015 and 2017, respectively. He is currently working towards a Ph.D. degree at KU Leuven, Belgium and BME. His research interests include nonlinear system identification, optimization, and wireless communication.

Zsolt KOLLÁR obtained his Diploma in Electrical Engineering in 2008 from the Budapest University of Technology and Economics (BME). He received his Ph.D. degree in Electrical Engineering from BME in 2013. He is currently an Associate Professor at the Department of Measurement and Information Systems. Since 2016, he is the head of the MATLAB Laboratory. His research interests include digital signal processing, system identification, quantization effects, and wireless communication.